JOC The Journal of Organic Chemistry

Article

pubs.acs.org/joc

Why Do Five-Membered Heterocyclic Compounds Sometimes Not Participate in Polar Diels–Alder Reactions?

Luis R. Domingo,[†] Patricia Pérez,*[,‡] and Daniela E. Ortega[‡]

[†]Departamento de Química Orgánica, Universidad de Valencia, Dr. Moliner 50, E-46100 Burjassot, Valencia, Spain

[‡]Facultad de Ciencias Exactas, Departamento de Ciencias Químicas, Laboratorio de Química Teórica, Universidad Andrés Bello, Av. República 275, 8370146 Santiago, Chile

Supporting Information

ABSTRACT: The reactions of bicyclic enone (BCE, **1**) with cyclopentadiene (Cp, **2**) and the five-membered heterocyclic compounds (FHCs) furan **3** and *N*-methyl pyrrole **4** for the construction of polycyclic heterocyclic compounds have been studied at the B3LYP/6-31G* level. No reaction takes place in the absence of Lewis acid (LA) catalysts as a consequence of the high activation energy associated with these reactions. Electrophilic activation of BCE **1** by formation of a complex with the BF_3 LA, **1**-BF_3, and solvent effects favor the reactions. However, a different reactivity is manifested by Cp **2** and FHCs **3** and **4**. Thus, while the reaction of **1**-BF_3 with Cp **2** yields the expected *exo* [4 + 2] cycloadduct, the reactions of these FHCs yield Michael adducts. In any case, the reactions are characterized by the nucleophilic/electrophilic interaction between the most nucleophilic centers of these dienes and the most electrophilic center of complex **1**-BF_3. The greater ability of FHCs **3** and **4** to stabilize positive charges opposed to Cp **2** favors a stepwise mechanism with formation of a zwitterionic intermediate. Although in most stepwise Diels–Alder reactions, the subsequent ring closure has unappreciable barriers, in these FHCs the abstraction of a proton with regeneration of the aromatic ring becomes competitive. Thermodynamic calculations suggest that the exergonic character of the formation of the Michael adducts could be the driving force for the reactions involving FHCs.

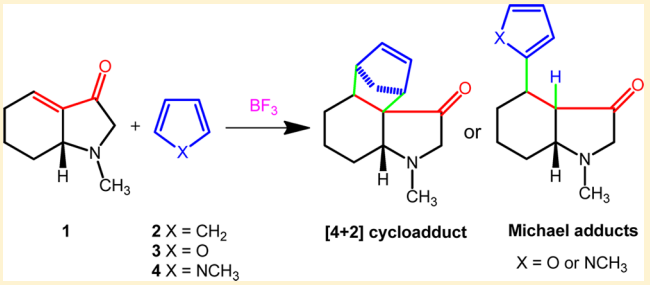

INTRODUCTION

The Diels–Alder (DA) reaction involving heterocyclic compounds is a powerful method for the construction of polycyclic heterocycles.[1] Five-membered heterocyclic compounds (FHCs), such as furans, pyrroles, and others are important reagents that participate in DA reactions as both diene or dienophile reagents.

Single FHCs can participate as diene components in DA reactions toward electrophilically activated π systems, due to their electron-rich nature, but do not readily participate as dienophilic components, demanding a chemical and/or physical activation for such a reaction. However, the presence of strong electron-withdrawing groups such as the nitro one activates FHCs electrophilically participating in DA reactions as the dienophilic component.[2]

Recently, Chau and Liu[3] studied experimentally the DA reactions of the fused nitrogen-containing bicyclic enone (BCE, **1**) with cyclopentadiene (Cp, **2**), furan **3**, and *N*-methyl pyrrole **4** as diene components in the construction of polycyclic heterocyclic compounds such as **5** (see Scheme 1). These DA reactions require the presence of BF_3 as Lewis acid (LA) catalyst to make the reactions feasible. Interestingly, two different reaction products were observed: [4 + 2] cycloadducts (CAs) such as **5-X** and/or Michael adducts (MAs) such as **6-X**, depending on the nature of the dienic component. Thus, in the case of BCE **1**, whereas Cp **2** yielded exclusively the [4 + 2] CA **5**, furan **3** and *N*-methyl pyrrole **4** yielded exclusively the MA **6** via aromatic electrophilic substitution (AES) reactions.[3]

Scheme 1

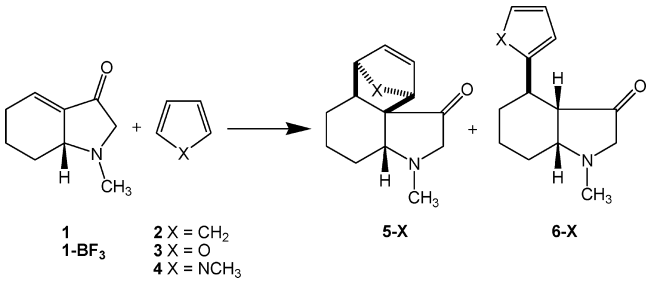

The participation of FHCs in DA reactions has been widely studied by theoretical methods. In 1995 Domingo, in collaboration with Jones, studied the DA reactions of several substituted vinylpyrroles **7a–d** with dimethyl acetylenedicarboxylate (DMAD) **8** (see Scheme 2).[4] Two different products were experimentally observed depending on the bulk group present in the vinyl substituents, i.e., [4 + 2] CAs such as **9**

Received: December 12, 2012
Published: January 25, 2013

dx.doi.org/10.1021/jo3027017 | J. Org. Chem. 2013, 78, 2462–2471

Scheme 2

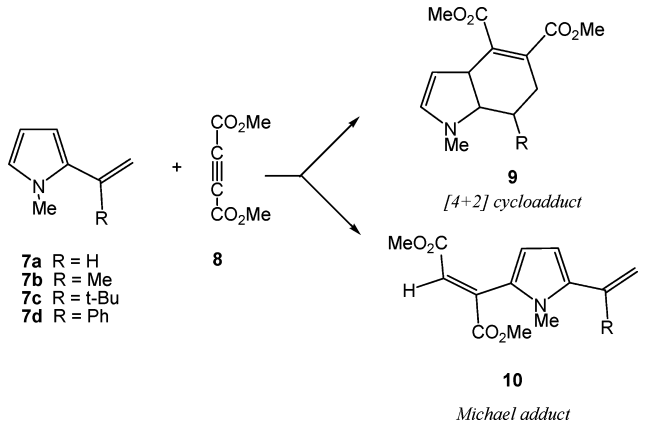

and/or MAs such as **10**.[5] An early semiempirical study of the reaction mechanisms provided an explanation for the formation of the two competitive compounds.[4a] While [4 + 2] CAs **9** originated from a high asynchronous cycloaddition process, MAs **10** came from an AES reaction in the pyrrole ring. Interestingly, the transition state structures (TSs) associated to the two competitive reactions were energetically and structurally similar, in clear agreement with the experiments. Later, Hartree−Fock and density functional theory (DFT) calculations using *N*-methyl pyrrole **4** enabled the establishment of stepwise mechanisms for the two competitive reactions, which share the first TS associated with the nucleophilic approach of **4** toward DMAD to yield the corresponding zwitterionic intermediate **11**.[6] Formation of [4 + 2] CA **12** or MA **13** is decided at the second step of the reaction (see Scheme 3).

Scheme 3

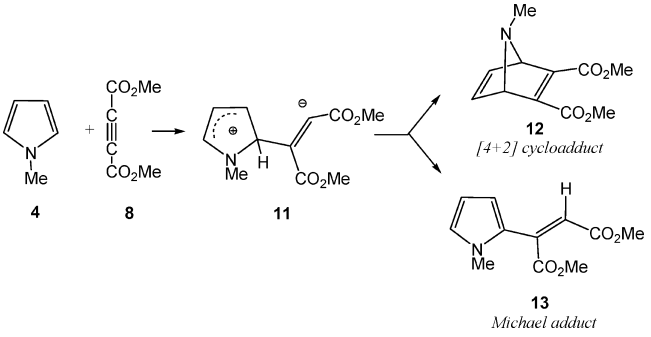

Jursic evaluated the reactivity of furan, pyrrole, and thiophene at the semiempirical level of theory.[7] Based on the frontier molecular orbital (FMO) theory, it was demonstrated that although the reaction with pyrrole is facilitated when compared with Cp and furan additions, experimental reactions with pyrrole are not feasible. Later, this author studied again the reactivity of pyrrole and its derivatives as dienes in DA reactions with acetylene derivatives as dienophiles, using a mix of semiempirical and hybrid density functional theories.[8] He found that furan is a reactive diene, thiophene is unreactive, and pyrrole fell in between the two. This trend in reactivity was attributed to the relative aromaticity of these compounds reflecting bond order uniformity in these heterocycles.

The DA reactions between cyclic five-membered dienes $(CH)_4X$, (X = CH_2, SiH_2, NH, PH, O, and S) and acetylene were studied by Sastry et al. at high level *ab initio* and DFT methods.[9] They found that the reaction of these compounds showed higher activation energies and higher exothermicities when compared to those using ethylene as a dienophile. Similar trends were obtained using butadiene as dienophile.[10]

Aromatic-controlled DA reactions were studied by Geerlings et al. using *ab initio* and DFT methods.[11] They found that while DA reactions involving quinodimethanes are both kinetically and thermodynamically favored by a progressive aromaticity gain during the reaction, in the DA reactions of anthracene and pentacene both are kinetically and thermodynamically unfavored due to the loss of aromaticity during the reaction.

Our group has studied the molecular mechanism of DA reactions for many years. A direct relationship between the decrease of the activation energy associated with the DA reaction and the charge transfer (CT) at the TSs was found.[12] This behavior enabled the characterization of polar Diels−Alder (P-DA) reactions.[13] In a P-DA reaction the increase of the electron-rich character of the diene (nucleophilicity), together with the increase of the electron-deficient character of the dienophile (electrophilicity), or *vice versa*, results in an enhancement of the CT that is accompanied by a lowering of the activation energy. In this context, electrophilicity[14] ω and nucleophilicity[15] N indices defined within the context of the conceptual DFT are powerful tools for the analysis of P-DA reactions. Interestingly, while furan **3** and pyrrole **4** display a larger nucleophilicity N index than Cp **2** (see later), they present low reactivity demanding more drastic reaction conditions such as high reaction temperatures or the use of LA catalysts.

Herein, the LA catalyzed reactions between the BCE **1** and the dienes **2**−**4** experimentally studied by Chau and Liu[3] are theoretically researched using DFT methods. The main interest of the current study is to establish the electronic behavior of FHCs such as furan **3** and *N*-methyl pyrrole **4**, which enable the formation of MAs adducts instead of the expected [4 + 2] CAs. The decisive role of LA catalysts in these reactions is analyzed.

COMPUTATIONAL DETAILS

DFT calculations were carried out using the B3LYP[16] exchange-correlation functional, together with the standard 6-31G* basis set.[17] Houk et al.[18] have examined many DA mechanisms and have reinforced that theoretical calculations using B3LYP functional with the 6-31G* basis set is appropriate to obtain reliable geometries and energies. Other recent studies carried out in P-DA reactions have also indicated that using large basis sets, including diffuse functions, do not improve the results obtained using the standard 6-31G* basis set.[13,19] The MPWB1K[20] hybrid meta functional to obtain reliable values of thermochemistry has been used (see later). Optimizations were carried out using the Berny analytical gradient optimization method.[21] Stationary points were characterized by frequency calculations in order to verify that TSs have one and only one imaginary frequency. Intrinsic reaction coordinate (IRC)[22] paths were traced in order to check the energy profiles connecting each TS to the two associated minima of the proposed mechanism using the second order González-Schlegel integration method.[23] Solvent effects of dichloromethane (DCM) were taken into account through full optimizations using the polarizable continuum model (PCM) as developed by Tomasi's group[24] in the framework of self-consistent reaction field (SCRF).[25] The electronic structures of stationary points were analyzed by the natural bond orbital (NBO) method.[26] All calculations were carried out with the Gaussian 09 suite of programs.[27]

The global electrophilicity index, ω, is given by the following simple expression,[14] $\omega = (\mu^2/2\eta)$, in terms of the electronic chemical potential μ[28] and the chemical hardness η.[28] Both quantities may be

dx.doi.org/10.1021/jo3027017 | J. Org. Chem. 2013, 78, 2462−2471

approached in terms of the one electron energies of the frontier molecular orbital HOMO and LUMO, ε_H and ε_L, as $\mu \approx (\varepsilon_H + \varepsilon_L)/2$ and $\eta \approx (\varepsilon_L - \varepsilon_H)$, respectively.[28] Recently, we have introduced an empirical (relative) nucleophilicity index,[15] N, based on the HOMO energies obtained within the Kohn–Sham scheme[29] and defined as $N = E_{HOMO}(Nu) - E_{HOMO}(TCE)$. Nucleophilicity refers to tetracyanoethylene (TCE), as it presents the lowest HOMO energy in a large series of molecules already investigated in the context of polar cycloadditions. This choice allows us to conveniently handle positive values for a nucleophilicity scale.[15a]

The electrophilic, P_k^+, and nucleophilic, P_k^-, Parr functions,[30] were obtained through the analysis of the Mulliken atomic spin density (ASD) of the radical anion and the radical cation by single-point energy calculations over the optimized neutral geometries using the unrestricted UB3LYP formalism for radical species. With these values at hand, local electrophilicity indices,[31] ω_k, and the local nucleophilicity indices,[32] N_k, were evaluated using the following expressions:[30] $\omega_k = \omega P_k^+$ and $N_k = N P_k^-$.

RESULTS AND DISCUSSION

Analysis of the Global and Local Reactivity Indices at the Ground States of the Reagents. Recent studies carried out on DA reactions have shown that the reactivity indices defined within the conceptual DFT are powerful tools for establishing the polar character of these reactions. In Table 1 the static global properties, including the electronic chemical potential (μ), chemical hardness (η), global electrophilicity (ω), and global nucleophilicity, N, in eV, for BCE **1**, complex **1-BF$_3$**, Cp **2**, furan **3**, and *N*-methyl pyrrole **4** are displayed.

Table 1. Electronic Chemical Potential, μ, Chemical Hardness, η, electrophilicity ω, and Nucleophilicity N Values, in eV, for the Series of Dienes and Dienophiles Shown in Scheme 1

compounds	μ	η	ω	N
1-BF$_3$	−0.17	0.14	2.89	2.66
1	−0.13	0.17	1.47	3.17
Cp **2**	−0.11	0.20	0.83	3.36
furan **3**	−0.10	0.24	0.58	3.01
N-methyl pyrrole **4**	−0.08	0.25	0.32	3.70

The electronic chemical potentials of Cp **2**, μ = −0.11 eV, furan **3**, μ = −0.10 eV, and *N*-methyl pyrrole **4**, μ = −0.08 eV, are higher than that of BCE **1**, μ = −0.13 eV, and complex **1-BF$_3$**, μ = −0.17 eV, indicating that the CT along the corresponding reactions will take place from these electron rich dienes toward BCE **1** and complex **1-BF$_3$**.

The electrophilicity of BCE **1** is ω = 1.47 eV, being classified as a strong electrophile on the electrophilicity scale.[33] On the other hand, **1** also has a high nucleophilicity index, N = 3.17 eV, and thus also is classified as a strong nucleophile on the nucleophilicity scale.[34] This ambiphilic behavior is a consequence of the presence of the enone and amine groups inside BCE **1**. Coordination of LA BF$_3$ to the oxygen atom of BCE **1** noticeably increases the electrophilicity of complex **1-BF$_3$**, ω = 2.89 eV, and slightly decreases its nucleophilicity, N = 2.66 eV.

As expected, the dienes present low electrophilicity ω values, 0.83 eV (**2**), 0.58 eV (**3**), and 0.32 eV (**4**). Thus, while Cp **2** is classified as a moderate electrophile, furan **3** and *N*-methyl pyrrole **4** are classified as marginal electrophiles. On the other hand, these dienes have high nucleophilicity N values, 3.36 eV (**2**), 3.01 eV (**3**), and 3.70 eV (**4**), being classified as strong nucleophiles. Note that furan **3** is the lowest nucleophile of these dienes due to the strong electronegative character of the oxygen atom.

The polar character of a cycloaddition process can be predicted using the electrophilicity difference of the reaction pair, $\Delta\omega$.[33] In this sense, the electrophilicity differences for complex **1-BF$_3$**, $\Delta\omega_{1\text{-}BF3/2}$ = 2.06 eV, $\Delta\omega_{1\text{-}BF3/3}$ = 2.31 eV, and $\Delta\omega_{1\text{-}BF3/4}$ = 2.57 eV, are higher than those with the isolated BCE **1**, $\Delta\omega_{1/2}$ = 0.89 eV, $\Delta\omega_{1/3}$ = 0.64 eV, and $\Delta\omega_{1/4}$ = 1.15 eV, clearly indicating that LA catalyzed processes will be more polar than uncatalyzed ones (see below).

Along a polar cycloaddition involving asymmetric reagents, the most favorable reactive channel is that involving the initial two-center interaction between the most electrophilic and nucleophilic center of both reagents.[35] Recently, we have proposed the electrophilic P_k^+ and nucleophilic P_k^- Parr functions derived from the excess of spin electron density reached via a global charge transfer process from the nucleophile to the electrophile.[30] Analysis of these functions accounts for the most favorable C–C bond formation via a C-to-C *pseudodiradical* coupling at the most electrophilic and nucleophilic centers of reagents. The P_k^+ and P_k^- Parr functions,[30] the corresponding local electrophilicity indices[31] ω_k in eV of BCE **1** and complex **1-BF$_3$**, and the local nucleophilicity[32] N_k in eV, of Cp **2**, furan **3**, and *N*-methyl pyrrole **4** are given in Table 2.

Table 2. Electrophilic, P_k^+, and Nucleophilic, P_k^-, Parr Functions, Local Electrophilicity Indices, ω_k, in eV, of BCE 1 and Complex 1-BF$_3$, and local nucleophilicity indices, N_k, in eV, of Cp 2, Furan 3, and *N*-Methyl Pyrrole 4

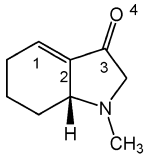

1
1-BF$_3$

2 X = CH_2
3 X = O
4 X = NCH_3

		P_k^+	ω_k			P_k^-	N_k
1	C1	0.49	0.72	**2**	C5	0.47	1.59
	C2	0.00	0.00		C6	0.08	0.27
	C3	0.27	0.40		C7	0.08	0.27
	O4	0.22	0.32		C8	0.47	1.59
1-BF$_3$	C1	0.51	1.47	**3**	C5	0.49	1.47
	C2	−0.11	−0.32		C6	0.07	0.21
	C3	0.44	1.27		C7	0.07	0.21
	O4	0.16	0.45		C8	0.49	1.47
					O9	−0.07	−0.20
				4	C5	0.52	1.92
					C6	0.07	0.26
					C7	0.07	0.25
					C8	0.52	1.92
					N9	−0.12	−0.43

Nucleophilic P_k^- Parr functions of Cp **2**, furan **3**, and *N*-methyl pyrrole **4** show symmetric nucleophilic activation at terminal centers C5 and C8. Interestingly, the O9 oxygen atom of furan **3** is deactivated, but the N9 nitrogen atom of *N*-methyl pyrrole **4** is strongly deactivated. This behavior is also reflected through the local N_k nucleophilicity indices of Cp **2**, furan **3**, and *N*-methyl pyrrole **4**, where a similar nucleophilic activation in the three C5═C6–C7═C8 dienic frameworks can be

dx.doi.org/10.1021/jo3027017 | J. Org. Chem. 2013, 78, 2462–2471

observed. The C5 and C8 centers are symmetrically activated, as a consequence of the symmetry present in these molecules. Negative values of N_k for the O9 oxygen of furan **3** and for the N9 nitrogen of *N*-methyl pyrrole **4** are in agreement with the local deactivation of these centers.

On the other hand, analysis of the electrophilic P_k^+ Parr functions of BCE **1** indicates that the C1 carbon, $P_k^+ = 0.49$, is more electrophilically activated than the C3 carbon, $P_k^+ = 0.27$, and the O4 oxygen, $P_k^+ = 0.22$. This behavior is consistent with the analysis of the local electrophilicity indices of BCE **1**, which indicates that the C1, $\omega_{C1} = 0.72$ eV, C2, $\omega_{C2} = 0.40$ eV, and O4, $\omega_{O4} = 0.32$ eV, atoms belonging to the enone framework are the most electrophilically activated centers. Note that the sum of the local electrophilicity of these atoms represents 97% of the global electrophilicity of BCE **1**. This analysis assigns the C1 carbon as the most electrophilic center of **1**. Consequently, along P-DA reactions between the nucleophilic dienes **2**−**4** and the electrophilic BCE **1**, the most favorable two-center interactions will take place between the C5 carbon of the dienes and the C1 carbon of BCE **1**, in clear agreement with the asynchronicity found at the corresponding TSs (see below).

Analysis of the local electrophilicity indices of complex **1**-BF_3 indicates that, after coordination of BF_3 LA to the carbonyl oxygen atom of BCE **1**, the C1 carbon remains as the most electrophilic center. However, interestingly, the carbonyl carbon C3 atom has been more electrophilically activated than the C1, as a consequence of the electrophilic deactivation of the C2 carbon, shown by its negative electrophilic Parr function, which favors the electrophilic activation of the C3 carbon. Note that ω_{C2} has a negative value, −0.32 eV, as a consequence of the negative value of corresponding electrophilic Parr functions, $P_k^+ = -0.11$. Despite this behavior, the C1 carbon remains more electrophilically activated than the C3 atom.

Reactions of BCE 1 with Cp 2 and FHCs 3 and 4, in the Absence and Presence of BF_3. *DA Reactions of BCE 1 with Cp 2 and FHCs 3 and 4.* Due to the asymmetry of BCE **1**, four stereoisomeric channels are feasible for each of the three DA reactions. They are related to the *endo* and *exo* approach modes of the diene system of **2**−**4** relative to the oxygen atom of BCE **1** and the two facial approach modes of these dienes toward the C1−C2 double bond of the BCE **1**. As these DA reactions are completely diastereoselective, only the *endo* and *exo* channels associated with the *syn* approach of dienes with respect to the hydrogen present at the bridge carbon were studied (see Scheme 4). Analysis of the stationary points associated with these DA reactions indicates that they take place via a one-step mechanism; in consequence, two stereoisomeric TSs, named **TS-Xn** or **TS-Xx**, and the corresponding CAs **5-Xn** or **5-Xx** were located and characterized (see Scheme 4). The total and relative energies associated with the stationary points involved in the DA reactions between the BCE **1** and the dienes **2**−**4** are displayed in Table 3.

The B3LYP/6-31G(d) gas phase activation energies associated with these DA reactions are 22.0 kcal/mol (**TS-2n**), 19.1 kcal/mol (**TS-2x**), 26.2 kcal/mol (**TS-3n**), 26.8 kcal/mol (**TS-3x**), 36.9 kcal/mol (**TS-4n**), and 29.9 kcal/mol (**TS-4x**). On the other hand, while the DA reaction of BCE **1** with Cp **2** is exothermic by −8.8 kcal/mol, those associated with the reaction of FHCs furan **3** and *N*-methyl pyrrole **4** are endothermic by 6.2 and 20.4 kcal/mol.

Some conclusions can be inferred from these energies: (i) The activation energy associated with the DA reaction between BCE **1** and Cp **2** is too high to take place experimentally. Note that this energy is similar to that for the unfavorable DA reaction between Cp and ethylene, 19.0 kcal/mol. (ii) The activation energies associated with the DA reactions of BCE **1** with furan **3** and *N*-methyl pyrrole **4** are 7 and 11 kcal/mol more unfavorable than that for the reaction with Cp. These results emphasize the low reactivity of these FHCs in these DA reactions, despite their high nucleophilic character. (iii) There is a change in stereoselectivity in these DA reactions: while the reactions with Cp **2** and *N*-methyl pyrrole **4** are *exo* selective, the reaction with furan **3** is slightly *endo* selective. (iv) Finally, while formation of CA **4** is thermodynamically favorable, formation of the CAs **5** and **6** is very unfavorable.

The geometries of the TSs involved in these DA reactions are given in Figure 1. The lengths of the C1−C5 and C2−C8 forming bonds are 2.003 and 2.596 Å at **TS-2n**, 1.964 and 2.646 Å at **TS-2x**, 1.893 and 2.427 Å at **TS-3n**, 1.849 and 2.467 Å at **TS-3x**, 1.748 and 2.333 at **TS-4n**, and 1.688 and 2.255 Å at **TS-4x**. Some conclusions can be drawn from these geometrical parameters: (i) The asynchronicity in bond formation at the TSs measured by $\Delta d = d(C2-C8) - d(C1-C5)$ ranges from 0.59 at **TS-2n** to 0.68 at **TS-2x**, indicating that the TSs correspond to high asynchronous bond-formation processes. (ii) At these TSs, the bond formation at the conjugated C1 carbon of BCE **1** is more advanced than that at the C2 ones. (iii) The length of the C1-C5 forming bond decreases in the

Scheme 4

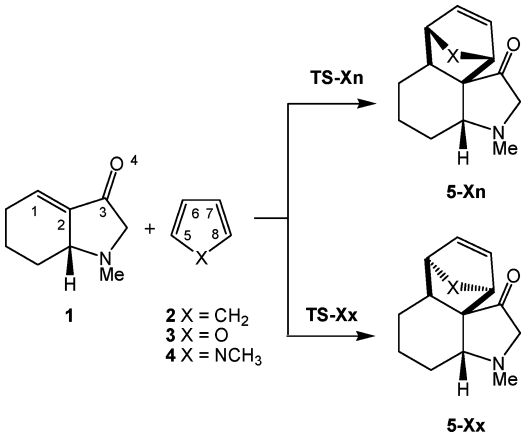

Table 3. Relative Energies (ΔE, in kcal/mol) of the Stationary Points Involved in DA Reactions of BCE 1 with Cp 2, Furan 3, and *N*-Methyl Pyrrole 4[a]

	ΔE
TS-2n	22.0
TS-2x	19.1
5−2n	−7.5
5−2x	−8.8
TS-3n	26.2
TS-3x	26.8
5-3n	6.2
5-3x	7.8
TS-4n	36.9
TS-4x	29.9
5-4n	16.6
5-4x	20.4

[a]Total energies for all stationary points are included in Supporting Information.

dx.doi.org/10.1021/jo3027017 | J. Org. Chem. 2013, 78, 2462−2471

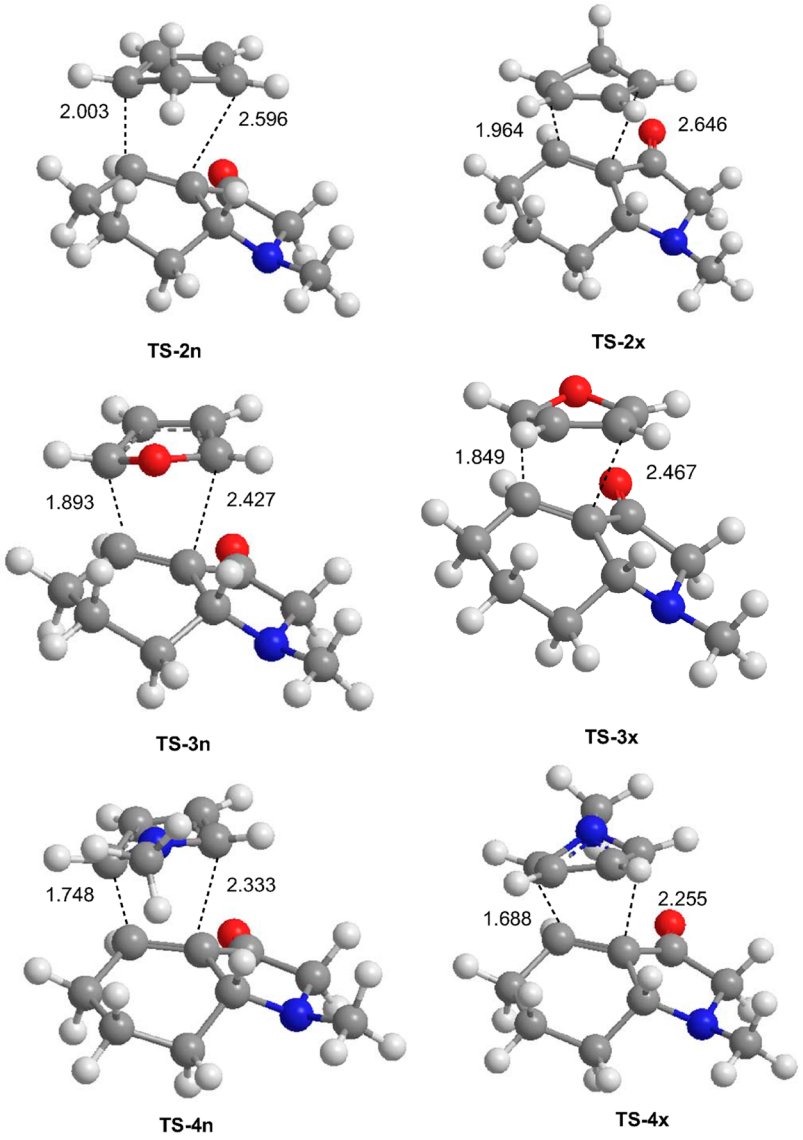

Figure 1. B3LYP/6-31G* geometries of the *endo* and *exo* regioisomeric TSs associated with of the stationary points involved in DA reactions of BCE **1** with Cp **2**, furan **3**, and *N*-methyl pyrrole **4**. Distances are given in Å.

order **2** > **3** > **4**, i.e., the more energetic the TS, the more advanced it is.

Finally, natural population analysis (NPA) allows us to evaluate the CT along these DA reactions. The natural atomic charges at the TSs were shared between BCE **1** and the dienes **2**−**4**. At the TSs, the CT that fluxes from the dienes to enone **1** is 0.16e at **TS-2n**, 0.16e at **TS-2x**, 0.21e at **TS-3n**, 0.21e at **TS-3x**, 0.30e at **TS-4n**, and 0.29e at **TS-4x**. There is an increase of the CT with the increase of the nucleophilic character of the diene. However, this behavior is not accompanied by a decrease of the activation energy, as expected in P-DA reactions.[13] The unfavorable activation energies associated with the DA reactions of the two FHCs can be related to the loss of the aromatic character of furan **3** and *N*-methyl pyrrole **4** on going from reagents to CAs. This is also evidenced by the endothermic character of these DA reactions.

In order to verify the assumption that the loss of aromaticity plays a relevant role in the unfeasibility of these DA reactions, the aromatic character of furan **3** and *N*-methyl pyrrole **4** was analyzed using the isodesmic reaction given in Scheme 5. B3LYP/6-31G(d) energy changes are displayed in Table 4. The aromatic character of benzene is also analyzed as reference aromatic compound.

Scheme 5

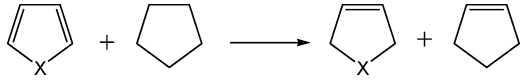

The endothermic character of these isodesmic reactions, related to the loss of the stabilization energy by resonance, is

Table 4. Energy Changes (Δ*E*, in kcal/mol) Associated with the Isodesmic Reactions of Scheme 5

compounds	Δ*E*
2, X = CH_2	3.0
3, X = O	22.0
4, X = NMe	29.9
benzene	38.0

dx.doi.org/10.1021/jo3027017 | *J. Org. Chem.* 2013, 78, 2462−2471

displayed in increasing order. The isodesmic energy involving Cp **2**, which is not aromatic, may be related to the loss of conjugation of the diene system. On the other hand, the computed isodesmic energy for benzene, 38.0 kcal/mol, is closer to the aromaticity experimentally estimated, 36 kcal/mol. From the isodesmic energies given in Table 4, it can be seen clearly that the aromaticity character increases in the order **3** < **4** < benzene.

These energy values indicate that furan **3** and *N*-methyl pyrrole **4** have a clear aromatic character when compared with the energy of conjugation of Cp **2**. Interestingly, the $\Delta\Delta E$ between the isodesmic reaction involving Cp **2** and those involving furan **3** and *N*-methyl pyrrole **4**, 19.0 and 26.9 kcal/mol, are closer to the $\Delta\Delta E_{reaction}$ in the DA reactions involving these FHCs with respect to that involving Cp **2**, 15.4 and 29.3 kcal/mol, respectively. Therefore, the increase of the corresponding activation energy and the decrease of the exothermic character in these DA reactions can be related to the increase of the aromatic character of these FHCs.

Remarkably, although the increase of the global nucleophilicity *N* indices of these FHCs does not match the activation energies, due to the unfavorable contribution associated with the loss of aromaticity, the nucleophilicity *N* predicts the increase of the polar character of the reaction measured by the CT at the TSs relative to the reaction with Cp **2** well.

Study of the LA Catalyzed Reactions of BCE 1 with Cp 2 and FHCs 3 and 4. Due to the high activation energies required for the DA reactions of BCE **1** with dienes **2**−**4**, the corresponding reactions must be experimentally LA catalyzed. Therefore, the reactions of complex **1**-BF_3, formed by coordination of the BF_3 LA to the carbonyl oxygen atom of BCE **1**, with dienes **2**−**4** were studied. An analysis of the stationary points involved in these LA catalyzed reactions indicates that formation of complex **1**-BF_3 displays a different behavior in the mechanisms of the reactions with Cp **2** and with FHCs **3** and **4**. Thus, while the reaction of complex **1**-BF_3 with Cp **2** takes place through a two-stage one-step mechanism via high asynchronous TSs, yielding *endo* and *exo* CAs **5**-BF_3 (see Scheme 6), the reactions with FHCs **3** and **4** take place through a stepwise mechanism, yielding formal [4 + 2] CAs or MAs (see Scheme 7). The energy changes in gas phase and in DCM associated with the stationary points of these LA catalyzed reactions are summarized in Table 5 and Supplementary Table S3. Since some stationary points involved in the competitive reactive channels have some zwitterionic character the discussion of the energetic results will based on DCM.

Scheme 6

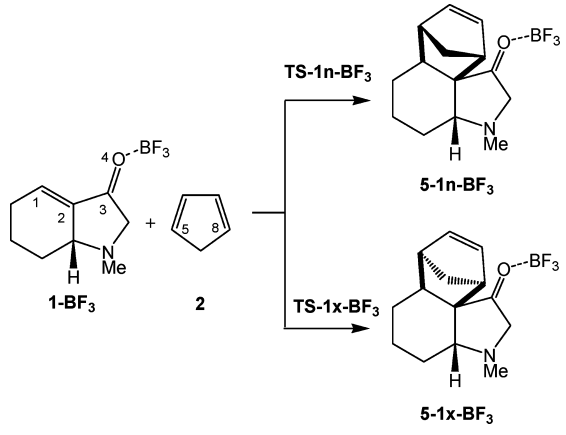

The energy barriers for the reactions of complex **1**-BF_3 with Cp **2** yielding the formal [4 + 2] CAs **5-2n**-BF_3 and **5-2x**-BF_3 are 11.1 (**TS-2n**-BF_3) and 9.0 (**TS-2x**-BF_3) kcal/mol, respectively. As for the uncatalyzed process, the *exo* channel is preferred by ca. 2 kcal/mol over the *endo* one, in clear agreement with the experimental result. It may be clearly seen that the energy barriers for the DA cycloaddition of complex **1**-BF_3 with Cp **2** are drastically reduced by *ca.* 10 kcal/mol (see Table 2). This DA reaction is exothermic by *ca.* −4 kcal/mol. Consequently, the presence of the LA BF_3 accelerates the reaction but does not alter its exothermic character. These findings are in complete agreement with experimental results by Chau and Liu, who found the *exo* [4 + 2] CA **5** (95%) when the reaction is treated with BF_3OEt_2/CH_2Cl_2 under mild conditions.[3] Also note that our results are in agreement with the global electrophilicity and nucleophilicity indices for both reagents (see Table 1).

The geometries of the TSs involved in these LA catalyzed DA reactions are given in Figure 2. The lengths of the C1−C5 and C2−C8 forming bonds are 1.976 and 2.949 Å at **TS-2n**-BF_3 and 1.973 and 2.953 Å at **TS-2x**-BF_3. The asynchronicity in bond formation at these TSs goes from 0.93 at **TS-2n**-BF_3 to 0.98 at **TS-2x**-BF_3, indicating that the TSs correspond to high asynchronous bond-formation processes associated to a two-stage one-step mechanism.

The CT from Cp **2** to **1**-BF_3 is 0.31e at **TS-2n**-BF_3, and 0.32e at **TS-2n**-BF_3. Note that these values are double when compared to the uncatalyzed processes. Therefore, coordination of LA BF_3 to BCE **1** causes the reaction to be faster via high asynchronous and polar TSs, as a consequence of the increased electrophilicity of complex **1**-BF_3.

More complex mechanisms are found for the reactions of complex **1**-BF_3 with FHCs furan **3** and with *N*-methyl pyrrole **4**, as a consequence of the formation of stable zwitterionic intermediates **IN1-Xy**-BF_3 after the nucleophilic approaches of **3** or **4** toward complex **1**-BF_3 (see Scheme 7). Previous theoretical studies have suggested that zwitterionic intermediates such as **IN1-Xy**-BF_3 are key species in stepwise DA reactions[6,36] and Michael additions[37] involving furans and pyrroles FHCs. The acronyms X = **3** or **4** referring to FHCs **3** or **4**, and y = n (*endo*) or x (*exo*) are used to simplify the nomenclature. As we mentioned in the Introduction, zwitterionic intermediates such as **IN1-Xy**-BF_3 can follow two competitive reaction channels (see Scheme 7): (i) along *channel I*, a ring-closure process allows for the formation of formal [4 + 2] CAs **5-Xy**-BF_3, via **TS2-Xy**-BF_3, and (ii) along *channel II*, a proton abstraction process promoted by a basic species give intermediates **IN2-X**-BF_3, which by a quick protonation, yields MAs **6-X**-BF_3.

The activation energies associated with the nucleophilic approaches of FHCs **3** and **4** toward complex **1**-BF_3 are 12.8 (**TS1-3n**-BF_3), 11.0 (**TS1-3x**-BF_3), 12.1 (**TS1-4n**-BF_3), and 6.4 (**TS1-4x**-BF_3) kcal/mol. Formation of the corresponding zwitterionic intermediates are endothermic by 12.3 (**IN1-3n**-BF_3), 11.0 (**IN1-3x**-BF_3), 10.9 (**IN1-4n**-BF_3), and 3.7 (**IN1-4x**-BF_3) kcal/mol. Consequently, coordination of BF3 LA to enone **1** noticeably decreases the activation energy associated with the nucleophilic approaches of FHCs **3** and **4** as a consequence of the remarkable increase of the electrophilic character of complex **1**-BF_3.

dx.doi.org/10.1021/jo3027017 | *J. Org. Chem.* 2013, 78, 2462−2471

Scheme 7

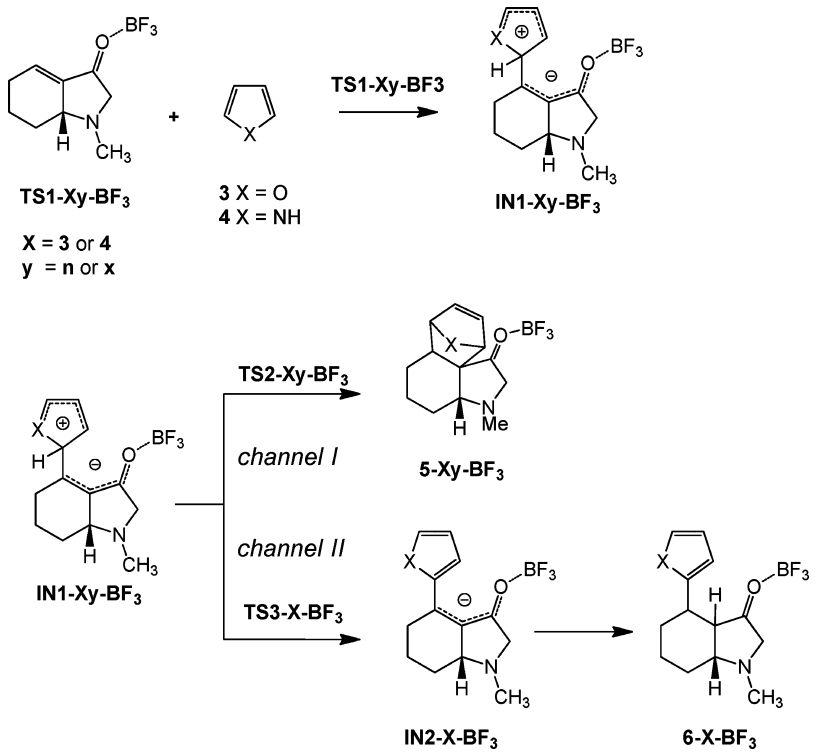

Table 5. Relative Energies (ΔE, in kcal/mol), in Gas Phase and in DCM, of the Stationary Points Involved in the *exo* Channels Associated with the Reactions of Complex 1-BF_3 with Cp 2, Furan 3, and *N*-Methyl Pyrrole 4[a]

	ΔE	
	gas phase	DCM
TS-2x-BF_3	10.7	9.0
5-2x-BF_3	−7.1	−4.7
5-2x	−8.9	−7.0
TS1-3x-BF_3	14.8	11.0
IN1-3x-BF_3	14.9	11.0
TS2-3x-BF_3	17.2	15.3
5-3x-BF_3	9.7	10.2
TS3-3-BF_3	8.9	6.9
5-3x	6.6	6.6
6-3	−15.6	−14.3
TS1-4x-BF_3	7.0	6.4
IN1-4x-BF_3	6.3	3.7
TS2-4x-BF_3	23.7	25.6
5-4x-BF_3	23.3	25.8
TS3-4-BF_3	10.2	15.2
5-4x	20.4	22.8
6-4	−12.4	−11.1

[a]Total energies for all stationary points are included in Supporting Information.

From these zwitterionic intermediates two competitive reaction channels are feasible: (i) along *channel I*, *endo* and *exo* [4 + 2] CAs **5-Xy-BF_3** are formed via **TS2-Xy-BF_3**, and (ii) along *channel II*, a proton abstraction process via **TS3-X-BF_3** regenerates the aromatic ring of these FHCs giving the anionic intermediate **IN2-X-BF_3**, which by a rapid protonation yields the final MAs **5-X-BF_3**. Note that the overall mechanism *via*

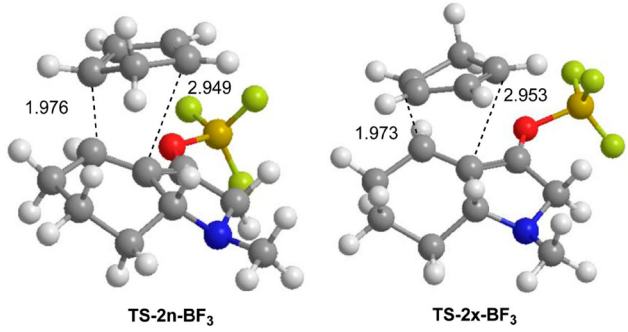

Figure 2. B3LYP/6-31G* geometries of the *endo* and *exo* regioisomeric TSs associated with of the stationary points involved in the DA reaction of complex **1-BF_3** with Cp **2**. Distances are given in Å.

channel II, corresponds to an AES in the aromatic ring of these FHCs.

Along *channel I*, the activation energies associated to the ring-closure processes from the corresponding intermediates **IN1-Xy-BF_3** are 2.2 (**TS2-3n-BF_3**), 4.3 (**TS2-3n-BF_3**), 18.2 (**TS2-4x-BF_3**), and 21.9 (**TS2-4x-BF_3**) kcal/mol. As the four **TS2-Xy-BF_3** are located above the TSs associated with the initial nucleophilic approaches, **TS1-Xy-BF_3**, the ring-closure step becomes the rate-determining step for the formation of the formal [4 + 2] CAs. The activation energies associated with these stepwise DA reactions are 14.5 (**TS2-3n-BF_3**), 15.3 (**TS2-3x-BF_3**), 29.1 (**TS2-4n-BF_3**), and 25.6 (**TS2-4x-BF_3**) kcal/mol. Formation of the corresponding formal [4 + 2] CA is endothermic by *ca.* 10 kcal/mol (**5-3x-BF_3**) and 26 (**5-4x-BF_3**) kcal/mol.

Channel II is initialized by a proton abstraction in the zwitterionic intermediates **IN1-Xy-BF_3** by a basic species. To model the proton abstraction processes, we have chosen

dx.doi.org/10.1021/jo3027017 | J. Org. Chem. 2013, 78, 2462−2471

dimethyl ether (DME) as a model of diethyl ether present in the reactions. In addition, as both *endo* and *exo* zwitterionic intermediates yield the same enolate intermediates, only the channels associated with *exo* **IN1-Xx-BF$_3$** were studied. From these intermediates, the activation energies associated with the proton abstractions are 6.9 (**TS3-3-BF$_3$**) and 15.2 (**TS3-4-BF$_3$**) kcal/mol. Formation of the final Michael adducts is exothermic by −14.2 (**6-3-BF$_3$**) and −11.1 kcal/mol (**6-4-BF$_3$**).

An analysis of the energetic results obtained for the three LA catalyzed reactions allows us to draw some interesting conclusions: (i) The LA catalyzed reaction of BCE **1** with Cp **2** affords only formal [4 + 2] CAs. (ii) This LA catalyzed DA reaction is markedly *exo* selective, in clear agreement with the experimental results. (iii) the LA catalyzed reaction of BCE **1** with FHCs **3** and **4** shows a more complex mechanism. After formation of a zwitterionic intermediate by the nucleophilic approaches of **3** or **4** to complex **1-BF$_3$**, two competitive reaction channels associated with a stepwise DA and an AES reaction emerge. (iv) For the LA catalyzed reaction of BCE **1** with *N*-methyl pyrrole **4**, the activation energy associated with the ring-closure step is very high, *ca.* 21.9 kcal/mol. Since the activation energy associated with the proton abstraction by DME is estimated to be 15.2 kcal/mol, energy results suggest that formation of the MA **6-4** is kinetically and thermodynamically favored with respect to formation of the formal [4 + 2] CA **5-4n**. Note that while formation of CA **5-4n** is endothermic by 19.2 kcal/mol, formation of MA **6-4-BF$_3$** is exothermic by −11.1 kcal/mol. (v) Analysis of the energy results for the LA catalyzed reaction of BCE **1** with furan **3** indicates a more complex scenario. Thus, whereas the kinetic data indicate that formation of the formal [4 + 2] CA **5-3n** via **TS2-3x-BF$_3$**, 4.3 kcal/mol, is favored with respect to formation of MA **6-3** via **TS3-3-BF$_3$**, 6.9 kcal/mol, the thermodynamic data indicate that while formation of the formal [4 + 2] CA **5-3x** is endothermic by 7.1 kcal/mol, formation of MA **6-3** is exothermic by −14.2 kcal/mol. Consequently, the B3LYP/6-31G* results suggest that the formation of the experimental MA **6-3** may take place via thermodynamic control.

Previous works have shown that the B3LYP functional is relatively accurate for kinetic data, although the reaction exothermicities are underestimated.[38] Recently, the Truhlar group has proposed some functionals, such as the MPWB1K,[20] which improve thermodynamic calculations. Therefore, in order to assert the aforementioned proposal, thermodynamic calculations for the formation of the formal [4 + 2] CA **5-3x** and the MA **6-3** were performed in DCM using the MPWB1K[20] hybrid meta functional. Relative energies and free energies are given in Table 6.

As shown in Table 6, MPWB1K/6-31G* calculations yield both competitive channels to be exothermic. However, when the thermal corrections to energies and entropies are included, while formation of formal [4 + 2] CA **5-3x** becomes endergonic, formation of MA **6-3** remains exergonic. Consequently, under equilibrium conditions, MA **6-3** will be the reaction product, in clear agreement with the experiments.

Table 6. MPWB1K Relative Energies (Δ*E*, in kcal/mol) and Relative Free Energies (Δ*G*, in kcal/mol) Computed at 273 K in DCM of Reagents and Products Involved in the LA Catalyzed Reaction of Enone 1 with Furan 3

	Δ*E*	Δ*G*
5-3	−8.9	7.6
6-3	−23.7	−8.5

The geometries of the TSs involved in the LA catalyzed reactions of BCE **1** with FHCs **3** and **4** are given in Figures 3 and 4. At the TSs associated with the nucleophilic approaches of furan **3** and *N*-methyl pyrrole **4**, the length of the C1−C5 forming bonds is 1.819 Å at **TS1-3n-BF$_3$**, 1.774 Å at **TS1-3x-BF$_3$**, 1.819 Å at **TS1-4n-BF$_3$**, and 1.911 Å at **TS1-4x-BF$_3$**, while the distances between the C2 and the C8 atoms are 2.927 Å at **TS1-3n-BF$_3$**, 2.906 Å at **TS1-3x-BF$_3$**, 3.308 Å at **TS1-4n-BF$_3$**, and 3.166 Å at **TS1-4x-BF$_3$**. A comparison of these geometrical parameters with those of the uncatalyzed processes shows the increase of the C2 and C8 distances as a consequence of the absence of any C2−C8 interaction during the first step of these stepwise processes.

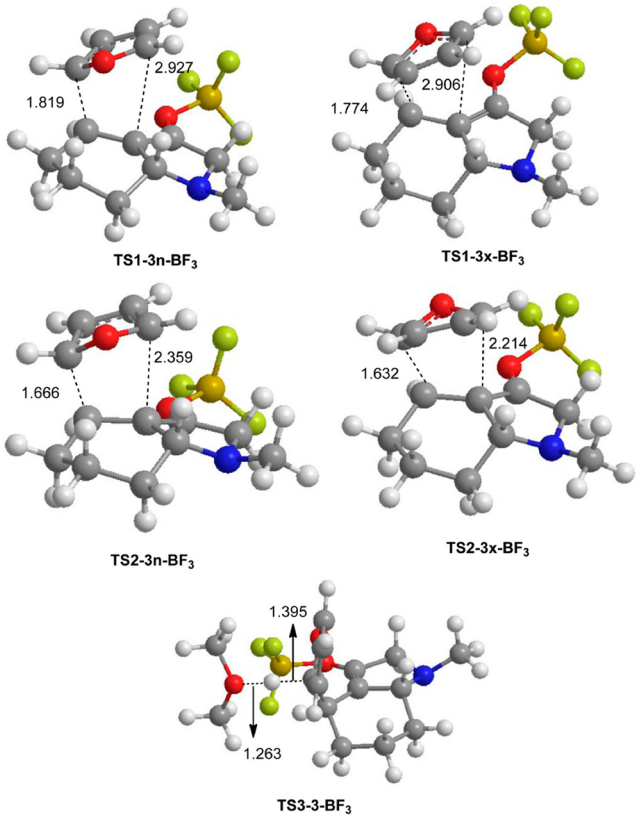

Figure 3. B3LYP/6-31G* geometries of the TSs associated with of the stationary points involved in reactions of complex **1-BF$_3$** with furan **3**. Distances are given in Å.

At the TSs associated with ring-closure step along *channel I*, the length of the C1−C5 bond is 1.666 Å at **TS2-3n-BF$_3$**, 1.632 Å at **TS2-3x-BF$_3$**, 1.644 Å at **TS2-4n-BF$_3$**, and 1.616 Å at **TS2-4x-BF$_3$**, while the length of the C2−C8 forming bond is 2.359 Å at **TS2-3n-BF$_3$**, 2.214 Å at **TS2-3x-BF$_3$**, 2.000 Å at **TS2-4n-BF$_3$**, and 1.908 Å at **TS2-4x-BF$_3$**. The length of the C1−C5 bond in these TSs indicates that it is already practically formed. On other hand, the short C2-C8 distance at the TSs associated with the ring closure of intermediates involving pyrrole **4**, indicate that they are more advanced than those involving furan **3**.

At the TSs involved in the proton abstraction process in intermediates **IN1-Xy-BF$_3$** along *channel II*, the lengths of the

dx.doi.org/10.1021/jo3027017 | J. Org. Chem. 2013, 78, 2462−2471

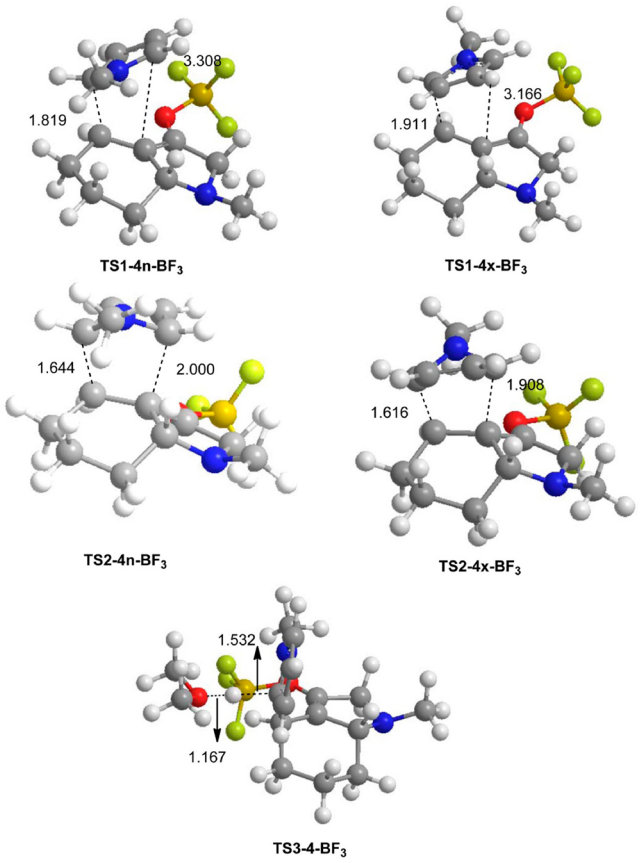

Figure 4. B3LYP/6-31G* geometries of the TSs associated with of the stationary points involved in reaction of complex **1-BF$_3$** with *N*-methyl pyrrole **4**. Distances are given in Å.

C−H breaking and H−O forming bonds are 1.395 and 1.263 Å at **TS3-3-BF$_3$** and 1.532 and 1.167 Å at **TS3-4-BF$_3$**.

Finally, at the TSs associated with the approach of nucleophilic furan **3** and *N*-methyl pyrrole **4** toward complex **1-BF$_3$**, the CT that fluxes from these aromatic dienes to **1-BF$_3$** is 0.42e at **TS1-3n-BF$_3$**, 0.43e at **TS1-3x-BF$_3$**, 0.53e at **TS1-4n-BF$_3$**, and 0.49e at **TS1-4x-BF$_3$**. Therefore, these polar reactions present a high CT at the TSs strong nucleophilic character of these FHCs.

CONCLUDING REMARKS

The reactions of BCE **1** with Cp **2** and the FHCs furan **3** and *N*-methyl pyrrole **4** for the construction of polycyclic heterocyclic compounds have been studied at the B3LYP/6-31G* level. Despite the strong nucleophilic character of Cp **2** and FHCs furan **3** and pyrrole **4**, no reaction takes place in the absence of LA catalysts. A consequence of this behavior is the high activation energy associated with these reactions mainly due to the low electrophilic character of BCE **1**.

Electrophilic activation of BCE **1** by formation of a complex with LA BF_3, **1-BF$_3$**, together with solvent effects, which stabilize zwitterionic species, favors these reactions. However, Cp **2** and both FHCs **3** and **4** show a different behavior toward **1-BF$_3$**. Thus, while the reaction of complex **1-BF$_3$** with Cp **2** takes place via a two-stage one-step mechanism, yielding the expected *exo* [4 + 2] CA, the reactions of these FHCs take place via a stepwise mechanism with formation of a zwitterionic intermediate, yielding MA products. In any case, the reactions are characterized by a nucleophilic/electrophilic two-center interaction between the most nucleophilic centers of these dienes, the extreme carbon of the diene systems, and the most electrophilic center of complex **1-BF$_3$**, the β conjugated position of the enone system. The larger capability to stabilize positive charges in the diene framework of these FHCs compared with Cp **2** favors the formation of the corresponding zwitterionic intermediates. Despite the subsequent ring closure having an unappreciable barrier in most stepwise Diels−Alder reactions, the loss of the aromatic character avoids this step in these FHCs, and a competitive channel associated with the abstraction of a proton with regeneration of the aromatic ring appears. Although this channel also presents an appreciable barrier in the reaction conditions, the overall reaction can be displaced toward the formation of the final MAs by a thermodynamic control; while formation of the formal [4 + 2] CAs is endergonic, formation of the MAs is exergonic. This complete DFT study permits the rationalization of the experimental outcomes.

ASSOCIATED CONTENT

Supporting Information

B3LYP/6-31G* total energies and Cartesian coordinates of the stationary points involved in reactions of BCE **1** with Cp **2**, furan **3**, and *N*-methyl pyrrole **4**, in gas and solution phases. MPWB1K total energies and total free energies computed at 273 K in DCM, of reagents and products involved in the LA catalyzed reaction of enone **1** with furan **3**. Complete citation for ref 27. This material is available free of charge via the Internet at http://pubs.acs.org.

AUTHOR INFORMATION

Corresponding Author

*E-mail: p.perez@unab.cl.

Notes

The authors declare no competing financial interest.

ACKNOWLEDGMENTS

This work has been supported by Fondecyt grant No. 1100278. L.R.D. also thanks Fondecyt for continuous support through Cooperación Internacional.

REFERENCES

(1) (a) Carruthers, W. *Some Modern Methods of Organic Synthesis*; 2nd ed.; Cambridge University Press: Cambridge, 1978. (b) Carruthers, W. *Cycloaddition Reactions in Organic Synthesis*; Pergamon: Oxford, 1990.

(2) (a) Della Rosa, C.; Kneetemen, M.; Mancini, P. M. E. *Tetrahedron Lett.* **2005**, *46*, 8711. (b) Della Rosa, C.; Kneetemen, M.; Mancini, P. M. E. *Tetrahedron Lett.* **2005**, *48*, 1435. (c) Brasca, R.; Kneetemen, M.; Mancini, P. M. E.; Fabian, W. M. F. *Eur. J. Org. Chem.* **2011**, 721.

(3) Chau, C.-M.; Liu, K.-M. *Org. Biomol. Chem.* **2008**, *6*, 3127.

(4) (a) Domingo, L. R.; Jones, R. A.; Picher, M. T.; Sepulveda-Arques, J. *Tetrahedron* **1995**, *51*, 8739. (b) Domingo, L. R.; Picher, M. T.; Andres, J.; Moliner, V.; Safont, V. S. *Tetrahedron* **1996**, *52*, 10693.

(5) (a) Jones, R. A.; Aznar-Saliento, T.; Sepúlveda-Arques, J. *J. Chem. Soc., Perkin Trans 1* **1984**, 2541. (b) Jones, R. A.; Sepúlveda-Arques, J. *Tetrahedron* **1981**, *37*, 1597.

(6) Domingo, L. R.; Picher, M. T.; Zaragoza, R. J. *J. Org. Chem.* **1998**, *63*, 9183.

(7) Jursic, B. S. *Can. J. Chem.* **1996**, *74*, 114.

(8) Jursic, B. S. *J. Mol. Struct. (THEOCHEM)* **1998**, *454*, 277.

(9) Vijaya, R.; Dinadayalane, T. C.; Sastry, G. N. *J. Mol. Struct. (THEOCHEM)* **2002**, *589*, 291.

(10) Dinadayalane, T. C.; Vijaya, R.; Smitha, A.; Sastry, G. N. *J. Phys. Chem. A* **2002**, *106*, 1627.
(11) Manoharan, M.; De Proft, F.; Geerlings, P. *J. Chem. Soc., Perkin Trans. 2* **2000**, 1767.
(12) (a) Domingo, L. R.; Arno, M.; Andres, J. *J. Org. Chem.* **1999**, *64*, 5867. (b) Domingo, L. R.; Aurell, M. J.; Pérez, P.; Contreras, R. *J. Org. Chem.* **2003**, *68*, 3884.
(13) Domingo, L. R.; Sáez, J. A. *Org. Biomol. Chem.* **2009**, *7*, 3576.
(14) Parr, R. G.; Von Szentpaly, L.; Liu, S. B. *J. Am. Chem. Soc.* **1999**, *121*, 1922.
(15) (a) Domingo, L. R.; Chamorro, E.; Pérez, P. *J. Org. Chem.* **2008**, *73*, 4615. (b) Domingo, L. R.; Pérez, P. *Org. Biomol. Chem.* **2011**, *9*, 7168.
(16) (a) Becke, A. D. *J. Chem. Phys.* **1993**, *98*, 5648−5652. (b) Lee, C.; Yang, W.; Parr, R. G. *Phys. Rev. B* **1988**, *37*, 785−789.
(17) Hehre, W. J.; Radom, L.; Schleyer, P. v. R.; Pople, J. A. *Ab initio Molecular Orbital Theory*; Wiley: New York, 1986.
(18) (a) Goldstein, E.; Beno, B.; Houk, K. N. . *J. Am. Chem. Soc.* **1996**, *118*, 6036. (b) Houk, K. N.; Gonzalez, J.; Li, Y. *Acc. Chem. Res.* **1995**, *28*, 81. (c) Houk, K. N.; Li, Y.; Evanseck, J. D. *Angew. Chem., Int. Ed. Engl.* **1992**, *31*, 682. (d) Borden, W. T.; Loncharich, R. J.; Houk, K. N. *Annu. Rev. Phys. Chem.* **1988**, *39*, 213.
(19) (a) Branchadell, V.; Font, J.; Moglioni, A. G.; Ochoa de Echagüen, C.; Oliva, A.; Ortuño, R. M.; Veciana, J.; Vidal-Gancedo, J. J. *Am. Chem. Soc.* **1997**, *119*, 9992. (b) Soto-Delgado, J.; Aizman, A.; Contreras, R.; Domingo, L. R. *Molecules* **2012**, *17*, 13687. (c) Rhyman, L.; Ramasami, P.; Joule, J. A.; Saez, J. A.; Domingo, L. R. *RSC Adv.* **2013**, *3*, 447.
(20) Zhao, Y.; Truhlar, G. D. *J. Phys. Chem. A* **2004**, *108*, 6908.
(21) (a) Schlegel, H. B. *J. Comput. Chem.* **1982**, *3*, 214−218. (b) Schlegel, H. B. In *Modern Electronic Structure Theory*; Yarkony, D. R., Ed.; World Scientific Publishing: Singapore, 1994.
(22) Fukui, K. *J. Phys. Chem.* **1970**, *74*, 4161−4163.
(23) (a) González, C.; Schlegel, H. B. *J. Phys. Chem.* **1990**, *94*, 5523−5527. (b) González, C.; Schlegel, H. B. *J. Chem. Phys.* **1991**, *95*, 5853−5860.
(24) (a) Tomasi, J.; Persico, M. *Chem. Rev.* **1994**, *94*, 2027−2033. (b) Simkin, B. Y.; Sheikhet, I. *Quantum Chemical and Statistical Theory of Solutions-A Computational Approach*; Ellis Horwood: London, 1995.
(25) (a) Cances, E.; Mennucci, B.; Tomasi, J. *J. Chem. Phys.* **1997**, *107*, 3032−3041. (b) Cossi, M.; Barone, V.; Cammi, R.; Tomasi, J. *Chem. Phys. Lett.* **1996**, *255*, 327−335. (c) Barone, V.; Cossi, M.; Tomasi, J. *J. Comput. Chem.* **1998**, *19*, 404−417.
(26) (a) Reed, A. E.; Weinstock, R. B.; Weinhold, F. *J. Chem. Phys.* **1985**, *83*, 735−746. (b) Reed, A. E.; Curtiss, L. A.; Weinhold, F. *Chem. Rev.* **1988**, *88*, 899−926.
(27) Frisch, M. J. et al. *Gaussian 09*; Gaussian, Inc.:, Wallingford, CT, 2009.
(28) (a) Parr, R. G.; Pearson, R. G. *J. Am. Chem. Soc.* **1983**, *105*, 7512. (b) Parr, R. G.; Yang, W. *Density Functional Theory of Atoms and Molecules*; Oxford University Press: New York, 1989.
(29) Kohn, W.; Sham, L. J. *Phys. Rev.* **1965**, *140*, 1133.
(30) Domingo, L. R.; Pérez, P.; Sáez, J. A. *RSC Adv.* **2013**, *3*, 1486.
(31) Domingo, L. R.; Aurell, M. J.; Pérez, P.; Contreras, R. *J. Phys. Chem. A* **2002**, *106*, 6871.
(32) Pérez, P.; Domingo, L. R.; Duque-Norena, M.; Chamorro, E. *J. Mol. Struct. (THEOCHEM)* **2009**, *895*, 86.
(33) Domingo, L. R.; Aurell, M. J.; Pérez, P.; Contreras, R. *Tetrahedron* **2002**, *58*, 4417.
(34) Jaramillo, P.; Domingo, L. R.; Chamorro, E.; Pérez, P. *J. Mol. Struct. (THEOCHEM)* **2008**, *865*, 68.
(35) Domingo, L. R.; Aurell, M. J.; Pérez, P.; Saez, J. A. *RSC Adv.* **2012**, *2*, 1334.
(36) (a) Yu, Z.-X.; Dang, Q.; Wu, Y.-D. *J. Org. Chem.* **2001**, *66*, 6029. (b) Griffith, G. A.; Hillier, I. H.; Moralee, A. C.; Percy, J. M.; Roig, R.; Vicent, M. K. *J. Am. Chem. Soc.* **2006**, *128*, 13130. (c) Domingo, L. R.; Aurell, M. J. *J. Org. Chem.* **2002**, *67*, 959.
(37) Kuniaki, I.; Shigehisa, K.; Kazuo, S. *Can. J. Chem.* **2009**, *87*, 760.
(38) (a) Check, C. E.; Gilbert, T. M. *J. Org. Chem.* **2005**, *70*, 9828−9834. (b) Jones, G. O.; Guner, V. A.; Houk, K. N. *J. Phys. Chem. A* **2006**, *110*, 1216. (c) Griffith, G. A.; Hillier, I. H.; Moralee, A. C.; Percy, J. M.; Roig, R.; Vicent, M. K. *J. Am. Chem. Soc.* **2006**, *128*, 13130.